



Imaging Features of Intramedullary Spinal Cord Lesions with Histopathological Correlation

Bhanupriya Singh¹  Abhishek Chauhan¹ Gaurav Raj¹

¹Department of Radiodiagnosis, Dr. Ram Manohar Lohiya Institute of Medical Sciences, Lucknow, Uttar Pradesh, India

Address for correspondence Bhanupriya Singh, MD, Department of Radiodiagnosis, Dr. Ram Manohar Lohiya Institute of Medical Sciences, Vibhuti Khand, Gomti Nagar, Lucknow, Uttar Pradesh, India, 226010 (e-mail: dr.singh.radiology@gmail.com).

Asian J Oncol

Abstract

Purpose Most of the intramedullary spinal cord lesions have a component of insidious myelopathic changes at the time of diagnosis. Among the spinal cord lesions, intramedullary neoplasms are rare (25%). They represent 4 to 10% of all central nervous system tumors. But due to involvement of tracts, they are associated with significant neurological symptoms. Their imaging features can help early diagnosis and predict prognosis. We aim to narrow down differential diagnoses of intramedullary lesions based on imaging findings.

Materials and Methods This retrospective study included 40 patients as a sample that underwent magnetic resonance imaging spine at our institution (on 3T machine). Patient population had varied clinical complaints, ranging from headache, nausea, vomiting, motor weakness, bladder and bowel involvement, progressive paraparesis to paraplegia. Lesions were evaluated site, size, margin, associated cysts, signal intensity, enhancement, and associated syringohydromyelia.

Results This study obtained majority of the lesions to be ependymoma (15) and astrocytoma (11), followed by infection (4), hemangioblastoma (3), and metastasis (2). Five patients were either lost to follow-up or not operated on.

Conclusion Most of the intramedullary lesions were malignant and were showing postcontrast enhancement. Ependymomas were more frequently present in cervical region, central in location with well-defined margins and focal postcontrast enhancement. Among the total of 15 ependymomas, three cases were associated with neurofibromatosis-2. Ependymomas were more frequently associated with syringohydromyelia and peripheral hemorrhage (cap sign). Astrocytoma was more frequently seen in children, thoracic and eccentric in location with ill-defined margins. Enhancement in astrocytoma was dependent on the grade of tumor. Metastasis was a differential, with imaging characteristics dependent on type of primary. Intramedullary granuloma due to infection can also be confusing mimics of neoplasm. High-velocity signal loss due to flow voids is seen in the hemangioblastomas.

Keywords

- ▶ spinal cord lesions
- ▶ MRI
- ▶ spinal cord lesions
- ▶ ependymoma
- ▶ astrocytoma
- ▶ metastasis
- ▶ granuloma

DOI <https://doi.org/10.1055/s-0042-1750792>.
ISSN 2454-6798.

© 2022. Spring Hope Cancer Foundation & Young Oncologist Group of Asia. All rights reserved.

This is an open access article published by Thieme under the terms of the Creative Commons Attribution-NonDerivative-NonCommercial-License, permitting copying and reproduction so long as the original work is given appropriate credit. Contents may not be used for commercial purposes, or adapted, remixed, transformed or built upon. (<https://creativecommons.org/licenses/by-nc-nd/4.0/>)

Thieme Medical and Scientific Publishers Pvt. Ltd., A-12, 2nd Floor, Sector 2, Noida-201301 UP, India

Introduction

Despite their rarity, intramedullary lesions hold diagnostic importance due to significant neurological compromise. Intramedullary neoplasms are rare, comprising 25% of the total spinal cord lesions. They represent 4 to 10% of all central nervous system tumors.¹ Their imaging characteristics help narrow down differential diagnosis and impact prognosis. On magnetic resonance imaging (MRI), these lesions present with cord enlargement, enhancement, and other features like syringohydromyelia, cysts, and hemorrhage.^{2,3} They hold high risk of neurologic deficits from the disease process as well as surgical interventions. Presenting complaints were dependent on location and extent of tumor; and the less preoperative neurologic deficit existing at presentation, the better the postoperative outcome was obtained. Hoshimaru et al found that the shorter the duration of symptoms, the better is the probability of long-term survival, prognosis, and postoperative outcome.^{4,5}

Materials and Methods

Image Acquisition

Images were acquired using GE SNIGMA 3T MR system imaging protocol that includes sagittal and axial T1-weighted and T2-weighted sequences and contrast-enhanced T1-weighted sequences in the sagittal, axial, and coronal planes. Short time inversion recovery (STIR) was added for the evaluation of intramedullary cord lesions as well as for the detection of bone abnormalities.

Statistical Analysis

All the results were analyzed with ratios and proportions.

Results

In the present study, we present data on the distribution of 40 patients with intramedullary spinal lesions with analysis. Clinical symptoms were directly proportional to size and site of spinal lesion. Diagnosis of most of the lesions was

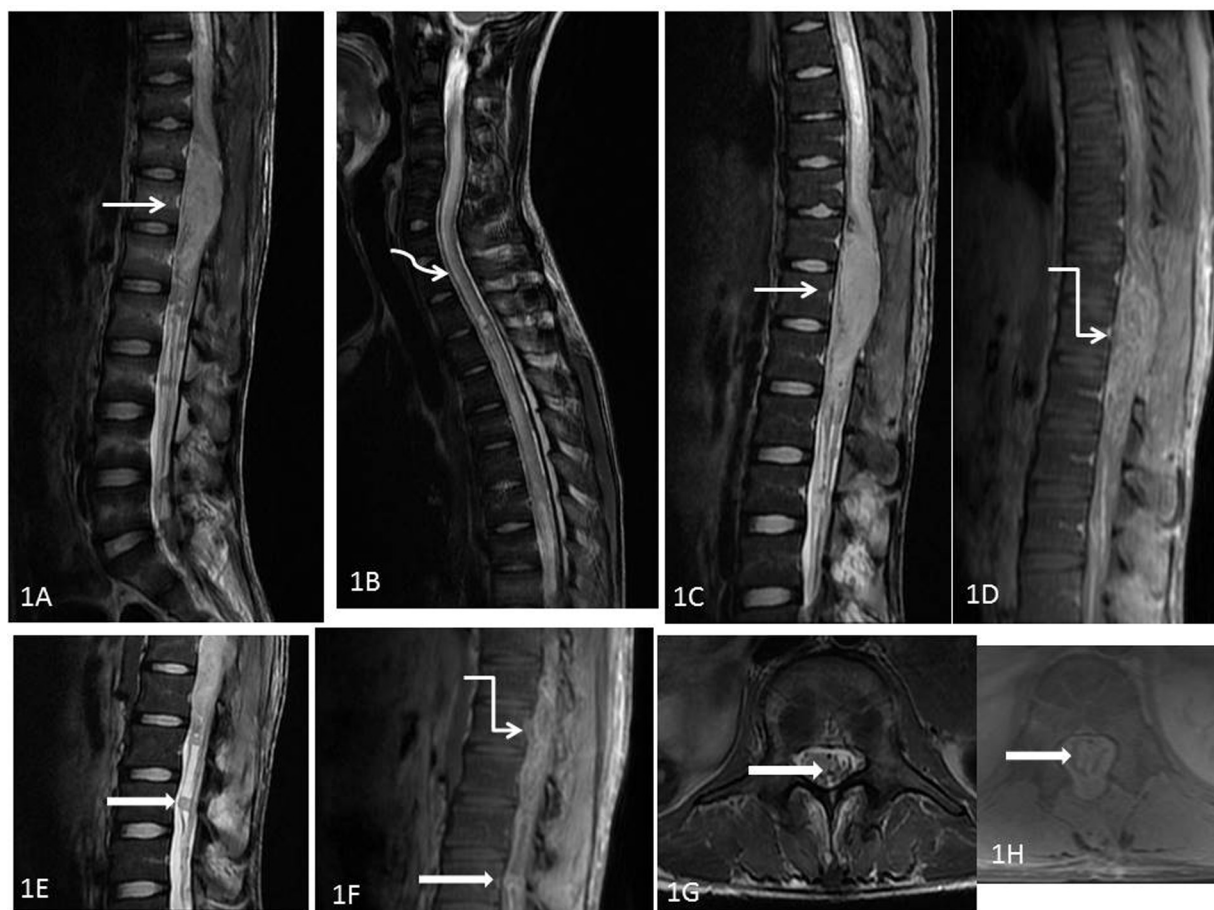


Fig. 1 Recurrent astrocytoma in a 19-year-old male presenting with paraplegia. Sagittal T2 (A and B) and short time inversion recovery (C) images showing diffuse hyperintense intramedullary lesion (white arrow) with long segment syrinx along cranial aspect (curved white arrow) (B). Adjacent postoperative and postradiotherapy changes noted. Sagittal postcontrast T1 (D and F) showing heterogeneous enhancement (white elbow arrow connector). Sagittal and axial T2 (E and G) and sagittal and axial postcontrast T1 (F and H) showing multiple similar intensity lesions (thick white arrow) with postcontrast enhancement noted in cauda equina region suggestive of drop metastasis.

confirmed on histopathology apart from five cases (12.5%) that either refused to get operated or were lost to follow-up. Astrocytomas (11 cases, 27.5%; ►Fig. 1) and ependymomas (15 cases, 37.5%; ►Figs. 2, 3) comprised of maximum cases, followed by two cases of metastasis (5%; ►Fig. 4), four cases of infective granuloma (10%; ►Fig. 5), and three cases of hemangioblastoma (7.5%; ►Chart 1, ►Table 1). There were 17 males (42%) and 23 females (58%; ►►Chart 2). There was wide age distribution, ranging from 2s to 84 years. However, maximum cases were seen in 10 to 20 years age group (►Chart 3). As observed on axial images, 31 cases (77%) were located centrally and 9 cases (23%) peripherally (►Chart 4). Average craniocaudal extent of lesions was around three vertebral segments, with wide range extending from 1 to 8 vertebral segments. Most of the cases were seen in cervical (23 cases, 57%), thoracic (13 cases, 32%) spine, followed by thoraco-lumbar (2 cases, 5%), lumbar (1 case, 3%), and sacral spine (1 case, 3%; ►Charts 5 and ►Chart 6; ►Table 2).

At least some form of enhancement was seen in 36 cases (90%) and no enhancement was seen in four cases (10%).

Intense focal enhancement was seen in 14 cases (35%) and diffuse enhancement was seen in 22 cases (55%; (►Charts 7 and ►Chart 8). Hemorrhage was present in 28 cases (70%) and no hemorrhage was present in 12 cases (30%). Classical T2 hypointense “Cap sign” was seen in 14 cases (35%; (►Figs. 2 and 3; ►Charts 9 and 10). Syringohydromyelia was present in 21 cases (52%; ►Chart 11). Well-defined sharp margins were seen in 32 cases (80%) and ill-defined blurred out margins were seen in 8 cases (20%; [►Chart 12]). Most of the lesions were iso- to hypointense on T1-weighted images, and hyperintense on T2 and STIR images (►Table 3). Cysts were commonly associated with the lesions. Nonenhancing plain cysts were seen in 22 cases (47%) and enhancing tumoral cysts were seen in 25 cases (53%; (►Chart 13).

Discussion

In an attempt to build community-based study on the spinal lesions in the region, medical records of tertiary care super-specialty center of North India, over a period of 3 years, are analyzed. Ependymomas are most common intramedullary

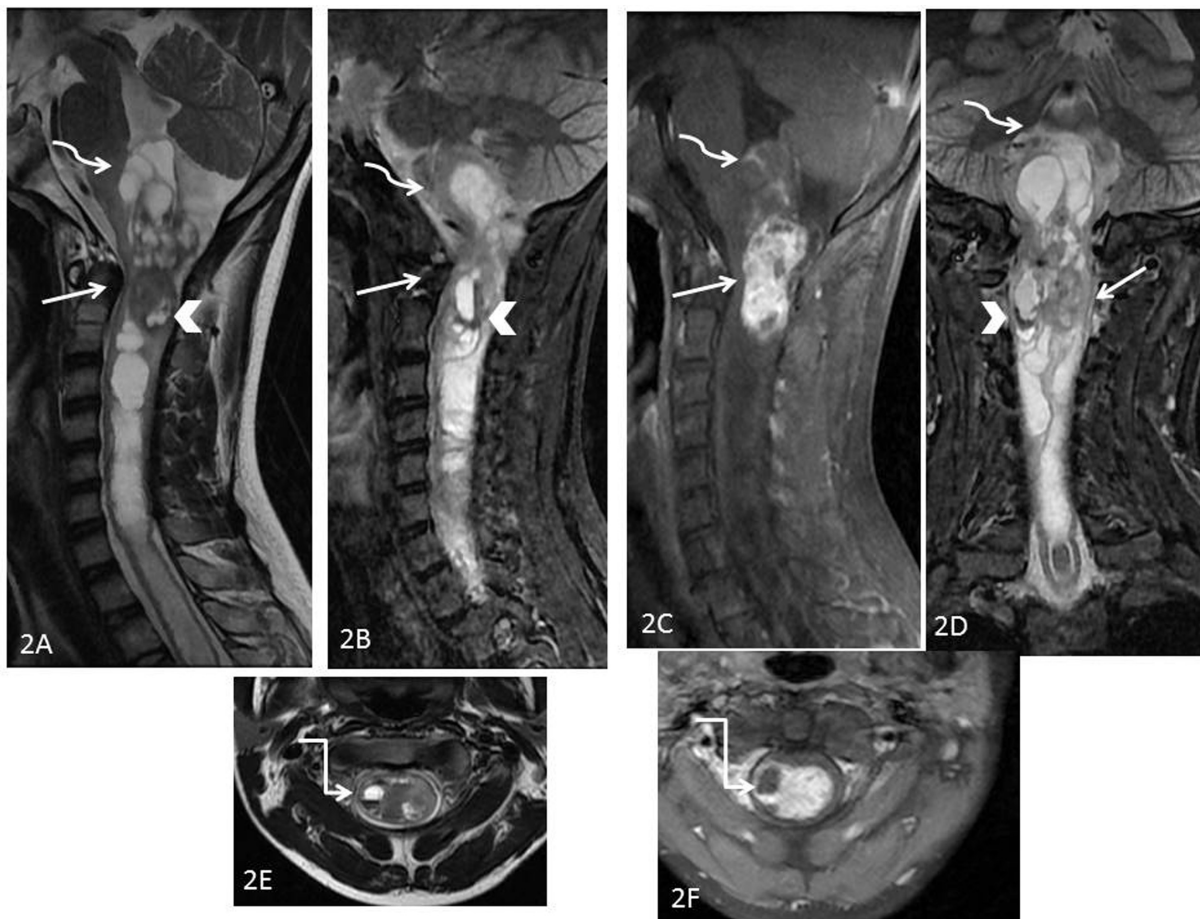


Fig. 2 Ependymoma in a 35-year-old male. Sagittal T2 (A) and short time inversion recovery (STIR) (B) post-contrast T1 (C) images showing moderately enhancing solid cystic heterogeneous hyperintense intramedullary lesion with internal foci of hemorrhage (white arrow). T2 hypointense rim noted along caudal aspect, giving “cap sign” (white arrowhead). Cranially it is reaching up to floor of fourth ventricle and compressing adjacent medulla (curved white arrow). Caudally it is compressing cord and causing complicated syrinx with septation. Coronal STIR image (D) confirms above findings with demarcation of craniocaudal extent. Well-defined nonenhancing cyst along caudal aspect of lesion, demonstrating “cap sign.” Axial T2 and post-contrast T1 (E and F) images confirm the above findings with nonenhancing cysts (white elbow arrow connector).



Fig. 3 Known case of ependymoma in a 18-year-old female. Sagittal T2 (A) and short time inversion recovery (B) postcontrast T1 (C) images show heterogeneous hyperintense intramedullary lesion with small intralesional cysts (white arrow). Cranially it is reaching up to medulla (curved white arrow). Axial T2 and postcontrast T1 (D and E) images confirm the above findings with nonenhancing cysts (white elbow arrow connector).

tumors in adult age group, and have association with neurofibromatosis-2. They are known to arise from ependymal lining of spinal cord and hence are seen more frequently central in location.^{6,7} Ependymomas have well defined margins, and are seen more frequently to compress the cord, rather than infiltrating it. At the junction of ependymoma and normal cord, the traversing vessels get stretched and eventually bleed. This leads to peripherally placed foci of hemorrhage, more prominent along craniocaudal margin, leading to “cap sign” (hypointense hemosiderin rim on T2-weighted images) in nearly 30% cases^{7,8} (► **Figs. 2 and 3**). Our findings were in accordance to Bhat et al in which the incidence of spinal cord primary and metastatic tumors in this province is approximately 0.2/100,000 persons per year for all ages. The malignant spinal cord tumors were found in 0.07/100,000 person per year.⁹ Brotchi and Fischer et al suggested that nontumoral (polar) cysts are associated with ependymoma more commonly than tumoral cysts. Tumoral cysts are usually intrasubstance that reflect necrosis, hemorrhage, or degeneration, which show inhomogeneous signal intensity and peripheral contrast enhancement

on MRI (► **Fig. 1**). Nonenhancing nontumoral (polar) cysts show cerebrospinal fluid (CSF) signal extends beyond the cranial or caudal pole of the neoplasm^{1,10} (► **Figs. 2 and 3**). Removal of nontumoral cysts can be skipped, and they can be aspirated, drained, or shunted, which allows for a smaller laminectomy needed to only resect the solid tumor portions.¹¹ Presence of syringohydromyelia is seen more consistently with ependymoma, than astrocytoma according to Kim et al. They defined syrinx as cystic cavity lined by gliotic parenchyma that arises outside the central canal. Ependymal-lined cystic central canal dilatation was referred as “hydromyelia.”^{12,13} However, due to overlapping features of syrinx and hydromyelia, combined term of syringohydromyelia has been used.^{14,15} Most of the ependymomas were T1 iso- to hypointense, with hyperintensity on T2 and STIR images, and homogenous intense postcontrast enhancement^{12,14,15} (► **Figs. 2 and 3**). Ependymomas tend to occur commonly in association with neurofibromatosis 2. Common location for the myxopapillary variant is in sacrococcygeal region and is believed to arise from either heterotopic ependymal cell rests or vestigial remnants of the distal



Fig. 4 Multiple metastasis in case of posterior fossa primary tumor (white arrowhead). Sagittal T2 (A) and postcontrast T1 (B) images showing heterogeneously enhancing intramedullary deposits (white arrow). Few smaller intradural enhancing deposits also noted in cervical cord (curved white arrow). Axial T2 (C) and axial postcontrast T1 (D) images show enhancing deposits along thoracic cord, closely abutting adjacent dura (white arrow).

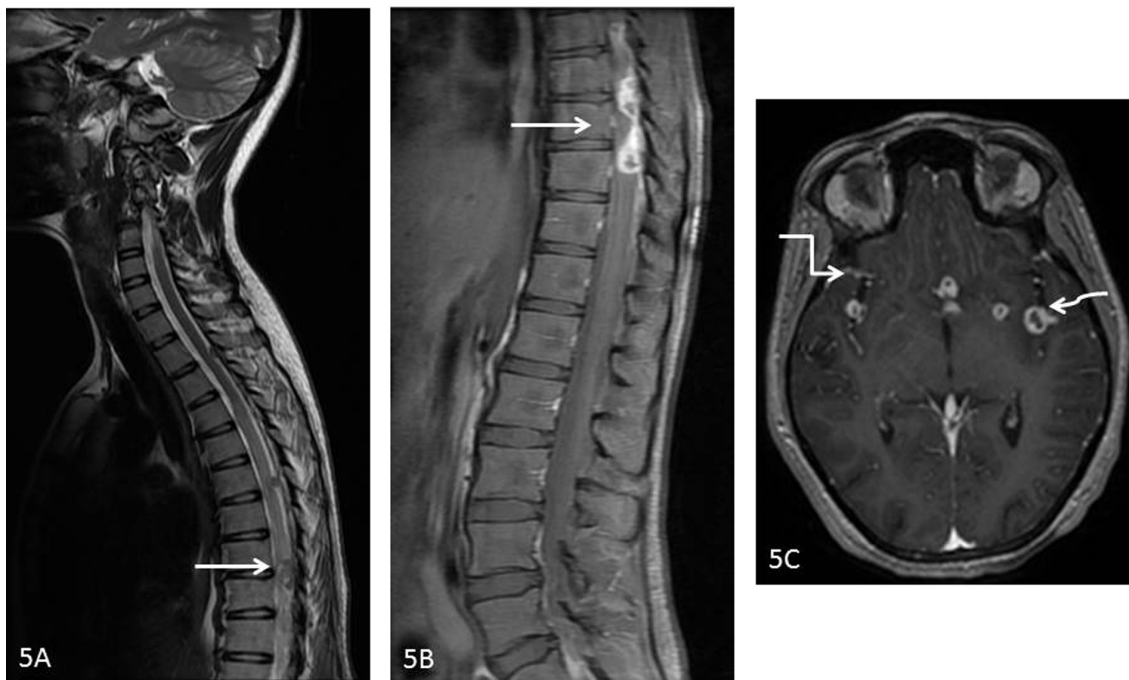


Fig. 5 Multiple tuberculomas in a 19-year-old female, presenting with seizures. Sagittal T2 (A) and postcontrast T1 (B) images of spine showing enhancing dural thickening along thoracic cord (white arrow) and nerve roots with adjacent cord edema. Axial postcontrast T1 (C) images of brain showing multiple ring-enhancing lesions in bilateral perisylvian region, left basifrontal, left gangliocapsular (curved white arrow) with meningitis (elbow arrow connector).

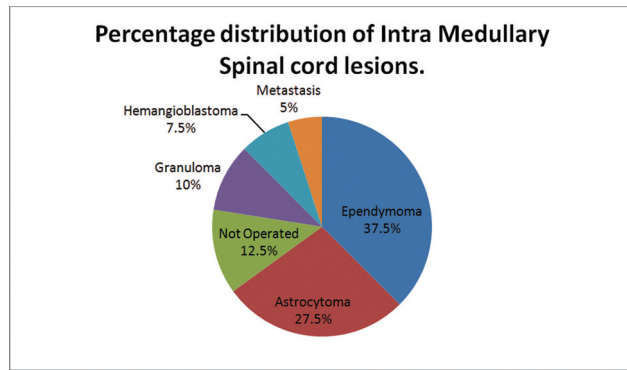


Chart 1 Percentage wise occurrence of intramedullary spinal cord lesions depicted by a pie chart.

Table 1 Distribution of intramedullary spinal cord lesions

Sr. No.	Spinal tumors	(Total, n = 40)
1	Ependymoma	15 (37.5%)
2	Astrocytoma	11 (27.5%)
3	Infective granuloma	4 (10%)
4	Hemangioblastoma	3 (7.5%)
5	Metastasis	2 (5%)
6	Not operated	5 (12.5%)

neural tube during canalization and retrogressive differentiation.^{15,16}

Astrocytomas are second most common intramedullary tumors, and most common among pediatric age group. They present with long multisegment (4–7 vertebral bodies) and holocord involvement pattern. Arising from astrocyte glial cells, they are known to be more cellular with ill-defined margins.^{14,16} Hence, they lack well-defined capsule or cleavage plane, making them prone for incomplete surgical resection and thereby recurrence. Astrocytomas are eccentric in

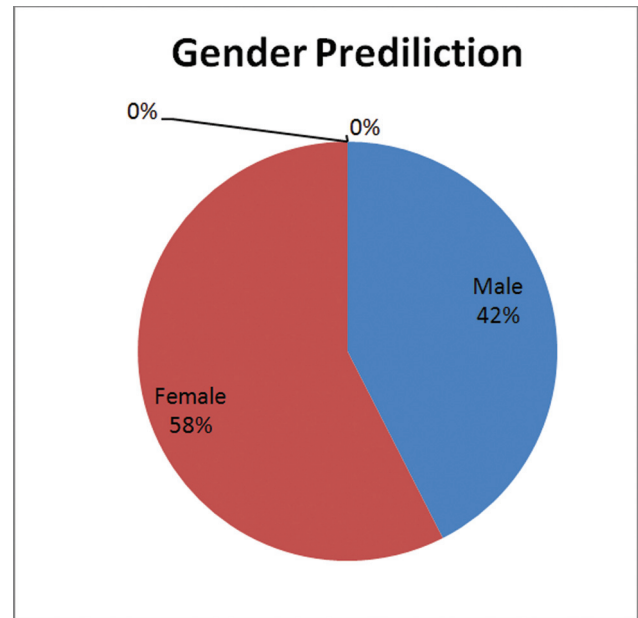


Chart 2 Gender distribution of intramedullary spinal cord lesions depicted by a pie chart.

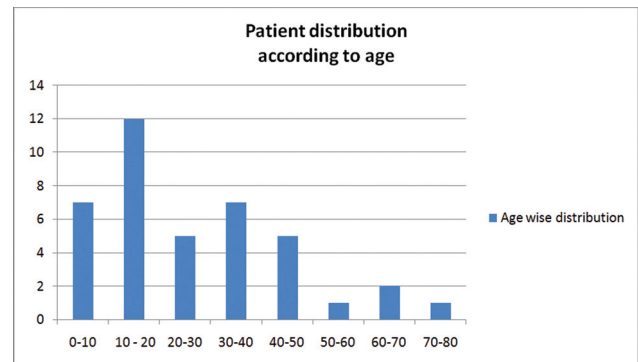


Chart 3 Age distribution of intramedullary spinal cord lesions depicted by a bar diagram.

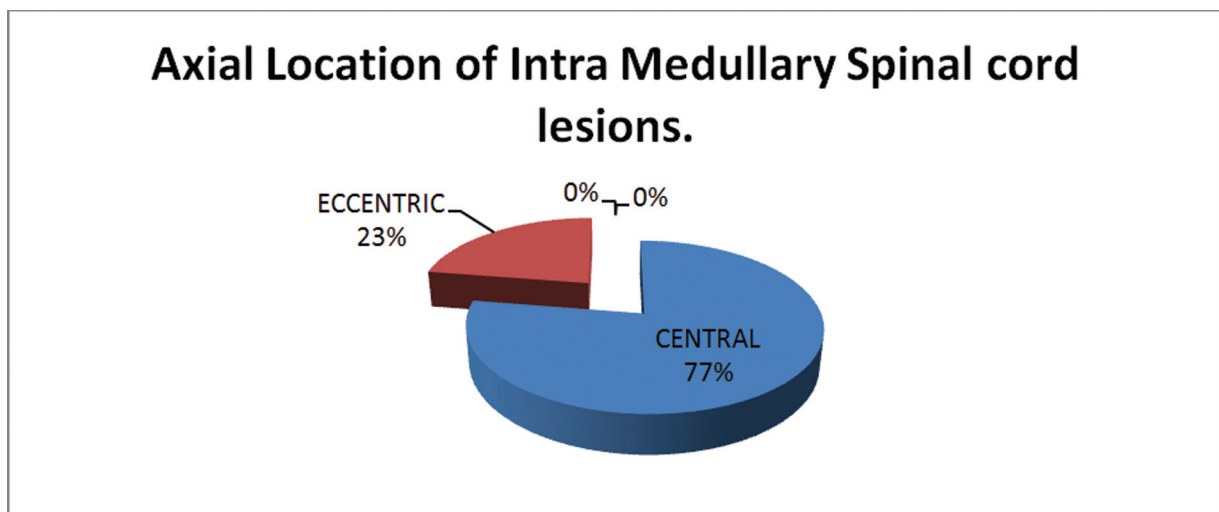


Chart 4 Pie chart showing percentage distribution of location of intramedullary spinal cord lesions, located axially with respect to central canal.

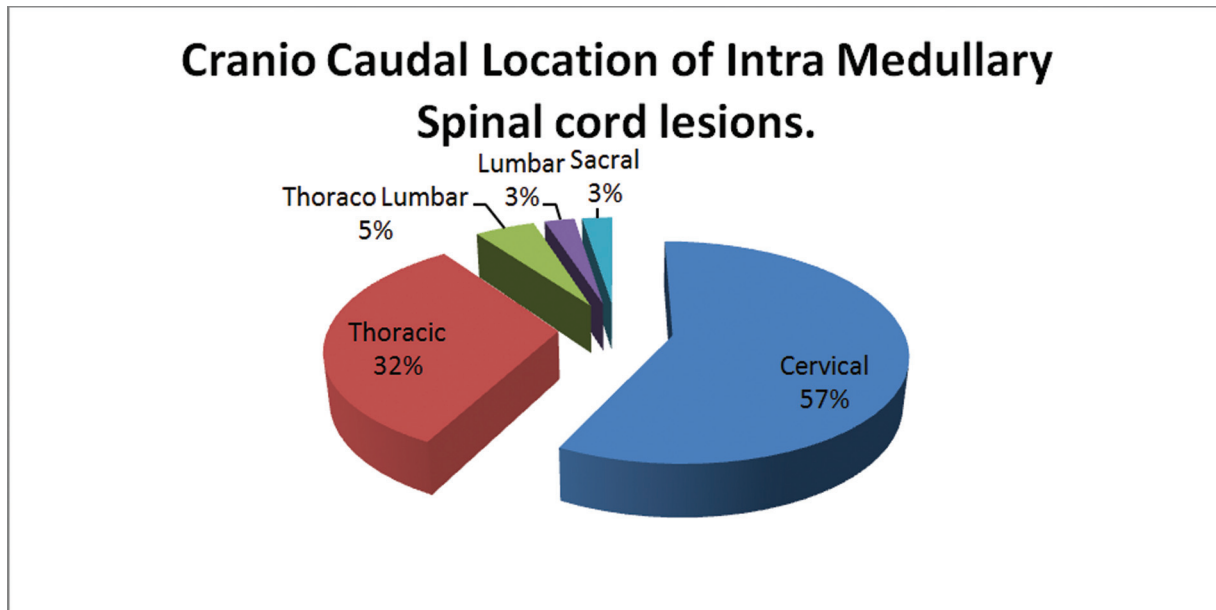


Chart 5 Pie chart showing percentage distribution of location of intramedullary spinal cord lesions, located vertically with respect to segment of spinal column.

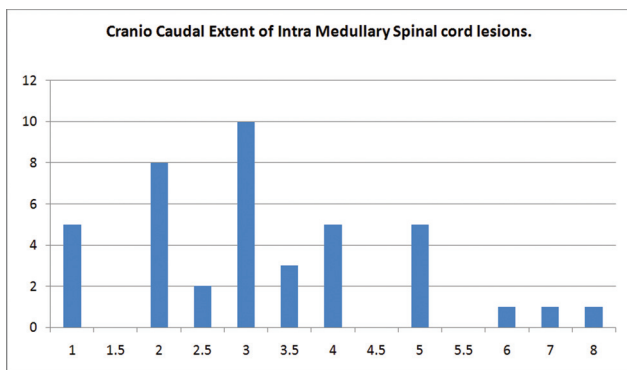


Chart 6 Bar diagram showing percentage distribution of location of intramedullary spinal cord lesions, located vertically with respect to segment of spinal column.

Table 2 Distribution of length of vertebral segment involved

Sr. No.	Length of vertebral Segment involved	Number of patients
1	1	5
2	2	8
3	2.5	2
4	3	10
5	3.5	3
6	4	5
7	5	5
8	6	1
9	7	1
10	8	1

location with the presence of associated cysts in approximately 30%.^{13,17} Astrocytomas associated with neurofibromatosis 1 tend to have lower grade (pilocytic astrocytoma) and most commonly involve thoracic location.^{12,14} They tend to have plane of dissection, and gross total resection can be attempted (► **Fig. 1**). However, higher grade astrocytomas are infiltrative, and complete resection without causing injury to the normal tissue is seldom accomplished.^{11,12} Therefore, conservative decompression, partial tumor removal, cyst decompression, and tissue diagnosis are commonly performed. In case of infiltrative residual or recurrent high-grade tumors, postoperative radiotherapy and chemotherapy are recommended. Their MRIs appear to expand the cord and are hypo- to isointense on T1-weighted images, hyperintense on T2 and STIR images, with varying degrees of patchy postcontrast enhancement.^{13,14} Differences between astrocytomas and ependymomas are compiled in ► **Table 4**.

Hemangioblastomas comprise of nearly 7% of all intramedullary neoplasms and show short segment involvement with prominent flow voids.¹⁸ They have cystic component with enhancing highly vascular nodular component. They have associated surrounding edema, syrinx and nearly one-third of them have association with Van Hippel Lindau disease.^{18,19}

Intramedullary spinal cord metastases are comparatively rare, especially in absence of known primary malignancy.²⁰ Drop metastasis can occur via CSF dissemination through the spinal cord, central canal, or contiguous spread from carcinomatous meningitis (► **Fig. 4**). Most common route of spread through hematogenous dissemination is either arterial or retrograde spread from the venous system. Presence of

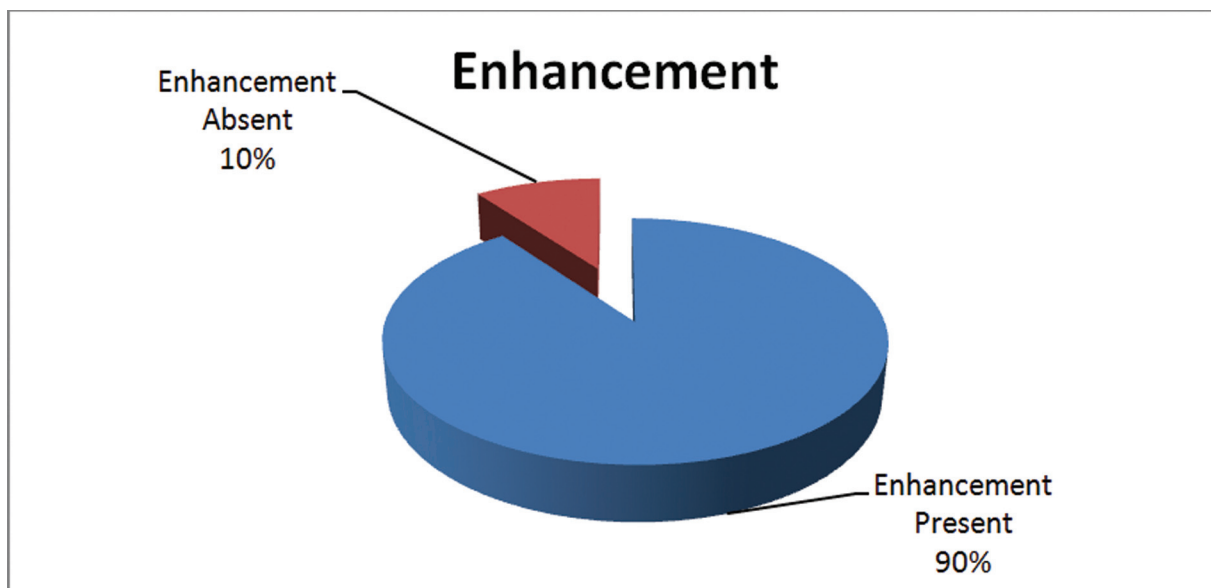


Chart 7 Pie chart showing percentage distribution of presence of enhancement in intramedullary spinal cord lesions.

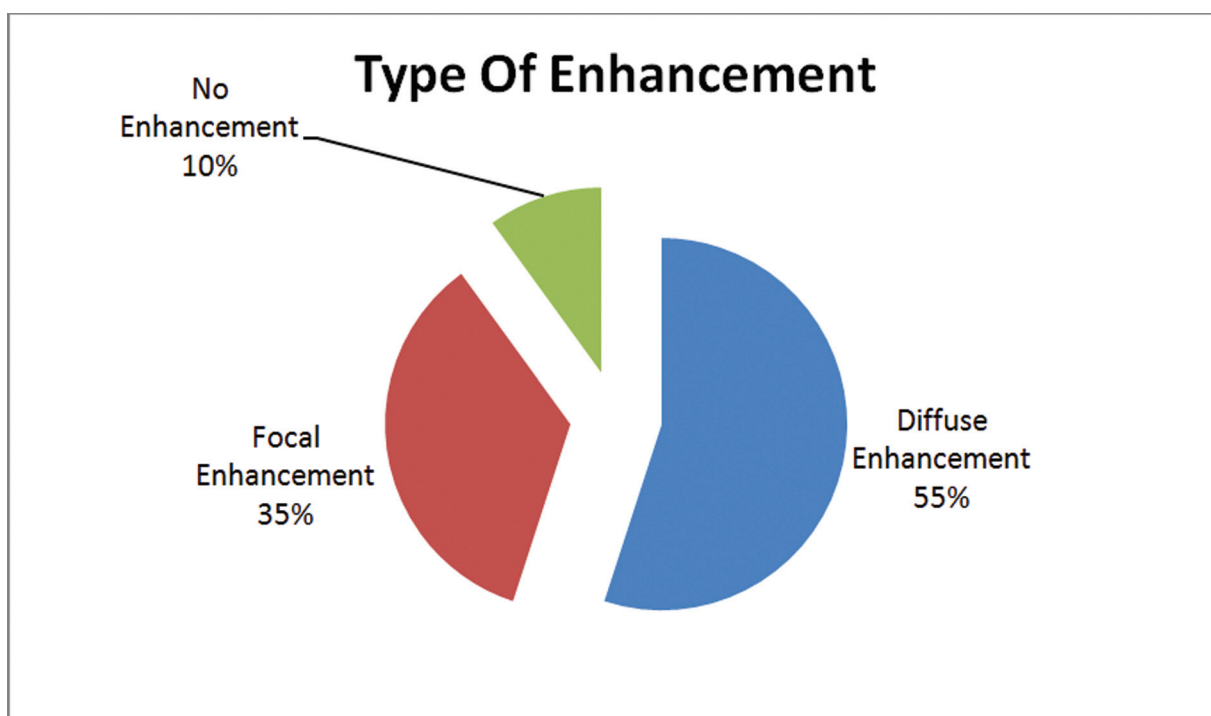


Chart 8 Pie chart showing percentage distribution of enhancement characteristics of intramedullary spinal cord lesions.

cystic change/hemorrhage makes their possibility unlikely. They show postcontrast enhancement with extensive edema for lesion size.^{20,21}

Infective granulomas presented as fusiform cord swelling with ill-defined iso- to hyperintensity on T1-weighted imaging (► Fig. 5). Surrounding edema maybe present with T2 hypointense area.²² Adjacent disc may show enhancement, depending on involvement. Varying amounts of caseous necrosis and liquefaction present as central hyperintensities.

An isohypointense rim, showing enhancement, was seen surrounding a hyperintense center.^{19,22}

Conclusion

Intramedullary lesions of cord are rare in general population and can be a diagnostic challenge. Hence, the onus of giving relevant and correct differential lies on the radiologist. They are associated with neurological compromise depending on

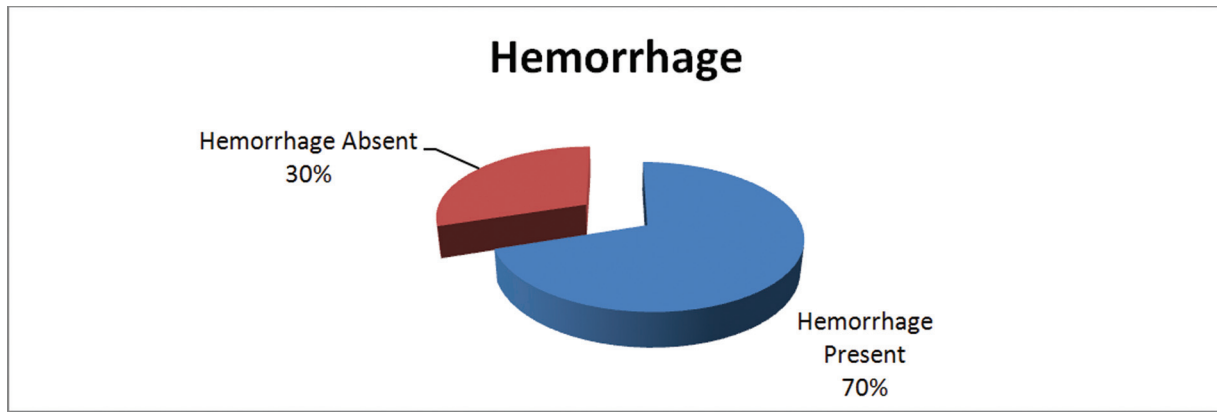


Chart 9 Pie chart showing percentage distribution of hemorrhage in intramedullary spinal cord lesions.

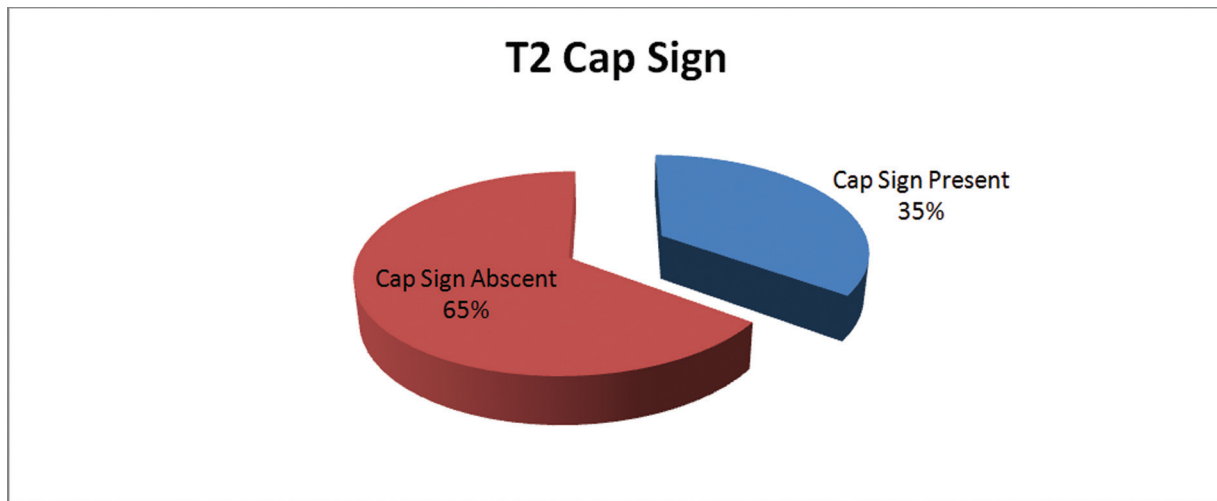


Chart 10 Pie chart showing percentage wise presence of T2 cap sign, secondary to hemorrhage in intramedullary spinal cord lesions.

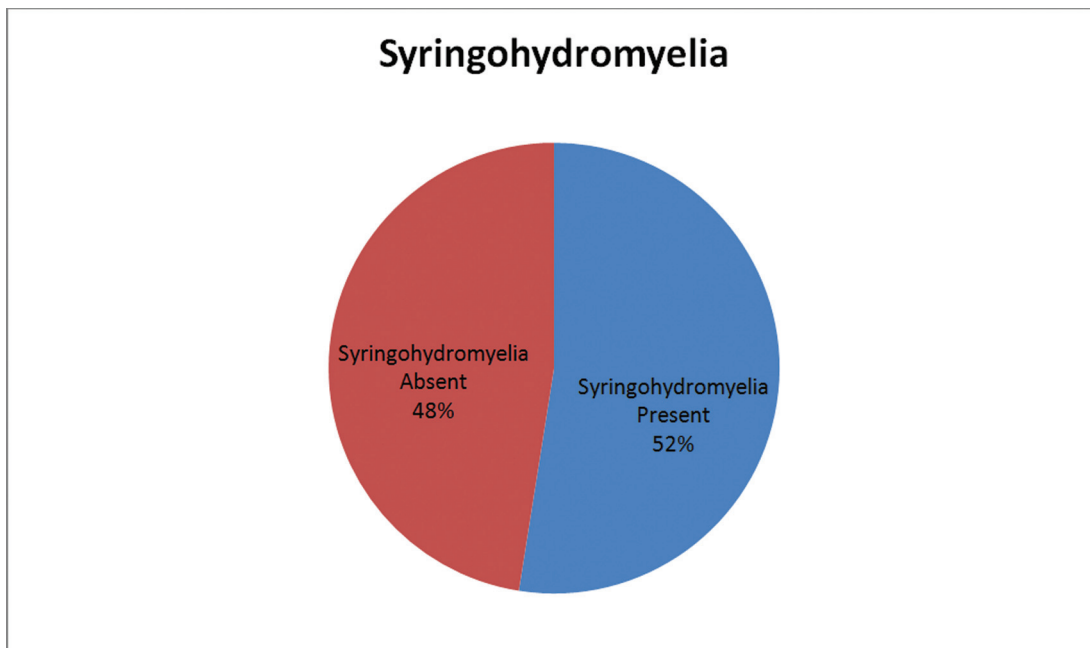


Chart 11 Pie chart showing percentage wise presence of syringohydromyelia, secondary to dilation of central canal in intramedullary spinal cord lesions.

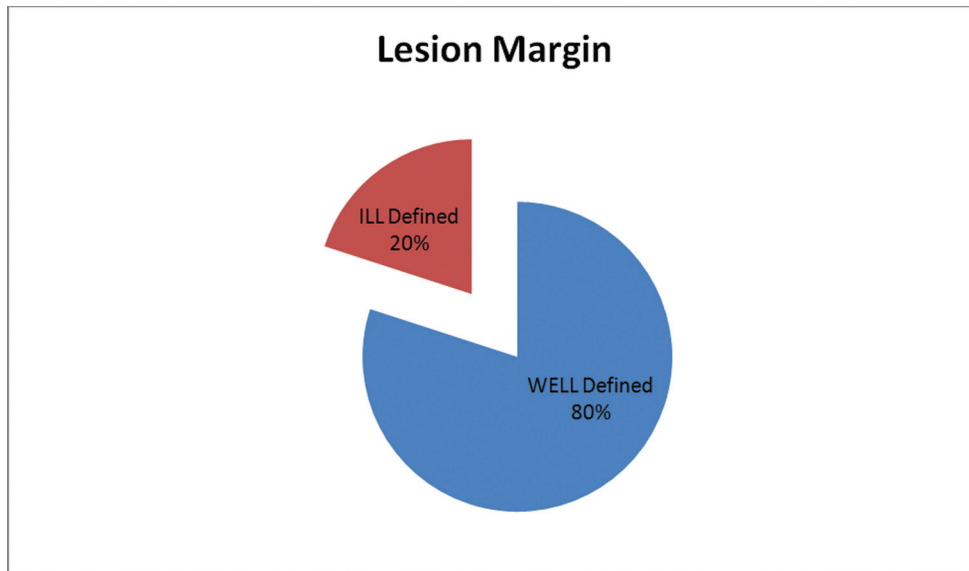


Chart 12 Pie chart showing percentage wise presence of type of margins in intramedullary spinal cord lesions.

Table 3 Distribution of MRI signal intensities

Sr. No.		Signal intensity	(Total, n = 40)
1	T1 signal intensity	T1 Hypointense	14 (35%)
2		T1 Isointense	24 (60%)
3		T1 Hyperintense	2 (5%)
4	T2 signal intensity	T2 Hypointense	1 (2.5%)
5		T2 Isointense	9 (22.5%)
6		T2 Hyperintense	29 (72.5%)
7	STIR signal intensity	STIR Hypointense	0
8		STIR Isointense	0
9		STIR Hyperintense	40 (100%)

Abbreviations: MRI, magnetic resonance imaging; STIR, short time inversion recovery.

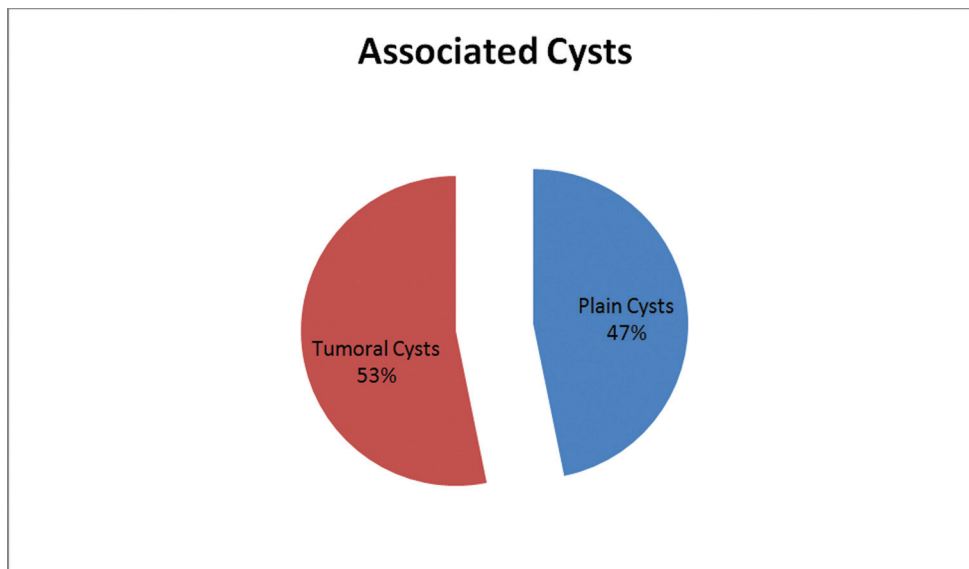


Chart 13 Pie chart showing percentage wise presence of type of peri tumoral cysts in intramedullary spinal cord lesions.

Table 4 Characteristics of Ependymoma and astrocytoma

Astrocytoma	Ependymoma
Common in pediatric (younger) population	Common in adult (older) population
Irregular or focal heterogenous enhancement	Focal or diffuse intense homogenous enhancement
Eccentric in location	Central in location
Ill-defined and infiltrative, poorly marginated	Well-defined and focal, sharply marginated
Average involvement: 6–7 vertebral segments	Average involvement: 3–4 vertebral segments
Thoracic more common than cervical	Cervical more common than thoracic
Large solid component	Small solid component
Complete resection generally not possible	Complete resection generally possible
Neurofibromatosis-1	Neurofibromatosis-2
Tumoral cysts common (eccentric and smaller, with irregular shape and postcontrast enhancement)	Nontumoral cysts common(polar)
Comparatively rare Hydrosyringomyelia, if present can be due to mass effect.	Commonly associated with Hydrosyringomyelia
Less common, intratumoral bleed maybe present.	Peripheral hemorrhage with “cap sign”
Bony changes less common.	Bony changes can be present (scoliosis/ canal widening)
More probability of residual lesion & residual neurological deficit	If resected, better prognosis.

size and site of lesion. Focusing on size, location, margin, cord expansion with narrowing of the surrounding CSF space signal intensity, pattern of contrast enhancement, presence of syringohydromyelia, tumoral cyst, nontumoral cyst, and hemorrhage offer a systematic approach to imaging interpretation of these conditions, and can greatly narrow the differential diagnosis.

Funding

None.

Conflict of Interest

None declared.

Acknowledgments

We would like to thank the Radiodiagnosis Department and Research Faculty for supporting this study.

Ethics Approval and Consent to Participate

Granted; OBSERVATIONAL STUDY. The patients' information was kept confidential.

Consent for Publication

The written informed consent was obtained from all research participants after a full explanation of the study.

Availability of Data and Materials

The datasets during and/or analyzed during the current study are available from the corresponding author on a reasonable request.

Authors' Contributions

BS was involved in conceptualization, design, the definition of intellectual content, literature search, clinical studies, experimental studies, data acquisition, data analysis, statistical analysis, manuscript preparation, and manuscript editing. GR contributed to designing, definition of intellectual content and literature search. AC was involved in definition of intellectual content, statistical analysis, manuscript editing, and manuscript review. All the authors contributed to study design, data collection, drafting of the manuscript, revision and reading of the manuscript and approved its final version.

Ethical Approval

This study was approved by Institutional Ethics Committee. All MRI examinations performed in the studies involving human participants were in accordance with the ethical standards of the Institutional Ethics Committee.

References

- Koeller KK, Rosenblum RS, Morrison AL. Neoplasms of the spinal cord and filum terminale: radiologic-pathologic correlation. *Radiographics* 2000;20(06):1721–1749
- Ledbetter LN, Leever JD. Imaging of intraspinal tumors. *Radiol Clin North Am* 2019;57(02):341–357
- Tomura N. [Imaging of tumors of the spine and spinal cord]. *Nippon Igaku Hoshasen Gakkai Zasshi* 2000;60(06):302–311
- Van Goethem JW, van den Hauwe L, Ozsarlak O, De Schepper AM, Parizel PM. Spinal tumors. *Eur J Radiol* 2004;50(02):159–176
- Seo HS, Kim JH, Lee DH, et al. Nonenhancing intramedullary astrocytomas and other MR imaging features: a retrospective study and systematic review. *AJNR Am J Neuroradiol* 2010;31(03):498–503

- 6 Abul-Kasim K, Thurnher MM, McKeever P, Sundgren PC. Intradural spinal tumors: current classification and MRI features. *Neuroradiology* 2008;50(04):301–314
- 7 Sun B, Wang C, Wang J, Liu A. MRI features of intramedullary spinal cord ependymomas. *J Neuroimaging* 2003;13(04):346–351
- 8 Miyazawa N, Hida K, Iwasaki Y, Koyanagi I, Abe H. MRI at 1.5 T of intramedullary ependymoma and classification of pattern of contrast enhancement. *Neuroradiology* 2000;42(11):828–832
- 9 Bhat AR, Kirmani AR, Wani MA, Bhat MH. Incidence, histopathology, and surgical outcome of tumors of spinal cord, nerve roots, meninges, and vertebral column - Data based on single institutional (Sher-i-Kashmir Institute of Medical Sciences) experience. *J Neurosci Rural Pract* 2016;7(03):381–391
- 10 Smith AB, Soderlund KA, Rushing EJ, Smirniotopoulos JG. Radiologic-pathologic correlation of pediatric and adolescent spinal neoplasms: Part 1, Intramedullary spinal neoplasms. *AJR Am J Roentgenol* 2012;198(01):34–43
- 11 Mohajeri Moghaddam S, Bhatt AA. Location, length, and enhancement: systematic approach to differentiating intramedullary spinal cord lesions. *Insights Imaging* 2018;9(04):511–526
- 12 Kim DH, Kim JH, Choi SH, et al. Differentiation between intramedullary spinal ependymoma and astrocytoma: comparative MRI analysis. *Clin Radiol* 2014;69(01):29–35
- 13 Nemoto Y, Inoue Y, Tashiro T, et al. Intramedullary spinal cord tumors: significance of associated hemorrhage at MR imaging. *Radiology* 1992;182(03):793–796
- 14 Lowe GM. Magnetic resonance imaging of intramedullary spinal cord tumors. *J Neurooncol* 2000;47(03):195–210
- 15 Murphey MD, Andrews CL, Flemming DJ, Temple HT, Smith WS, Smirniotopoulos JG. From the archives of the AFIP. Primary tumors of the spine: radiologic pathologic correlation. *Radiographics* 1996;16(05):1131–1158
- 16 Parmar HA, Ibrahim M, Castillo M, Mukherji SK. Pictorial essay: diverse imaging features of spinal schwannomas. *J Comput Assist Tomogr* 2007;31(03):329–334
- 17 Bourgouin PM, Lesage J, Fontaine S, et al. A pattern approach to the differential diagnosis of intramedullary spinal cord lesions on MR imaging. *AJR Am J Roentgenol* 1998;170(06):1645–1649
- 18 Asthagiri AR, Mehta GU, Zach L, et al. Prospective evaluation of radiosurgery for hemangioblastomas in von Hippel-Lindau disease. *Neuro-oncol* 2010;12(01):80–86
- 19 Sze G, Krol G, Zimmerman RD, Deck MD. Intramedullary disease of the spine: diagnosis using gadolinium-DTPA-enhanced MR imaging. *AJR Am J Roentgenol* 1988;151(06):1193–1204
- 20 Rykken JB, Diehn FE, Hunt CH, et al. Intramedullary spinal cord metastases: MRI and relevant clinical features from a 13-year institutional case series. *AJNR Am J Neuroradiol* 2013;34(10):2043–2049
- 21 Lv J, Liu B, Quan X, Li C, Dong L, Liu M. Intramedullary spinal cord metastasis in malignancies: an institutional analysis and review. *OncoTargets Ther* 2019;12:4741–4753
- 22 Lu M. Imaging diagnosis of spinal intramedullary tuberculoma: case reports and literature review. *J Spinal Cord Med* 2010;33(02):159–162